Energy transfer and Förster's dipole coupling approximation investigated in a real-time Kohn-Sham scheme

D. Hofmann, T. Körzdörfer, and S. Kümmel
Physikalisches Institut, Universität Bayreuth, D-95440 Bayreuth, Germany
(Received 19 April 2010; published 23 July 2010)

We present a scheme to investigate energy transfer by real-time propagation of the Kohn-Sham equations. The scheme's purpose is to check and go beyond the dipole coupling approximation underlying a Förster-type energy transfer, and to obtain information about the coupling on the grounds of the density-functional theory. We observe deviations from the dipole coupling approximation for small molecules.

DOI: 10.1103/PhysRevA.82.012509 PACS number(s): 31.15.ee, 31.70.Hq, 82.20.Rp, 82.20.Wt

I. ENERGY TRANSFER AND TIME-DEPENDENT DENSITY FUNCTIONAL THEORY

Energy transfer is one of the most fundamental processes on the molecular scale, governing light-harvesting in biological systems [1,2] and energy conversion in electronic devices such as organic solar cells [3–5] or light-emitting diodes [6]. The design principles of natural light-harvesting complexes [7–9] have found considerable interest, as hopes are high that the principles realized in nature can be mimicked in the design of artificial organic devices [3,10,11].

One standard method to interpret experimental data of excitation energy transfer between a donor (D) and an acceptor (A) molecule separated by the distance R is the so-called Förster resonance energy transfer (FRET) theory [9–21]. Förster theory describes the nonradiative energy transfer mediated by a (quantum-mechanical) coupling between the transition dipoles of the donor and acceptor molecules [13–15]. One of the central assumptions in FRET is that the coupling between D and A can be described by a (point)-dipole-dipole interaction, falling as $1/R^3$. Furthermore, FRET theory is formulated for the weak coupling regime (i.e., the isolated D and A excited states do not change significantly on coupling). Based on these assumptions Förster derived an expression for the energy transfer rate showing a characteristic R^{-6} distance dependence, with the nuclear vibrations being subsumed into a spectral overlap factor between donor emission and acceptor absorption spectra. The resulting, rather simple expression for the energy transfer rate, see Sec. II for details, allows for determining the intermolecular distance R by spectroscopy of the coupled D-A system, and D as well as A individually.

Thus, FRET has gained tremendous importance as it establishes a spectroscopic ruler on the nanoscale [22,23]. Typically it is applied in a range of distances from about 10 to 100 Å [24,25]. However, in recent years the applicability of the dipole coupling approximation underlying FRET has been questioned in many applications [25–33] as frequently the intermolecular distance R is comparable to the molecules' extension, or the D and A molecules are connected by bridging units.

Theoretical insight into the validity of the dipole coupling approximation is, therefore, of great importance. As the molecules of practical relevance often contain many electrons, (time-dependent) density functional theory (TD)DFT appears as a natural choice to study the problem on a first-principles scale at bearable computational cost. Recently, TDDFT has been applied to Förster-type excitation energy transfer questions [34–41] in the Casida-type linear response formalism [42]. As a complementary approach to the Casida formalism, real-time implementations [43–52] of TDDFT are finding increasing attention due to their accuracy and favorable scaling, which allows one to apply them to large systems [53–55]. In addition, they do not require computation of the exchange-correlation kernel, which can be advantageous when advanced functionals that explicitly employ the orbitals are used [47,49,56–58].

In the following we present a real-time TDDFT scheme for investigating energy transfer and the dipole coupling approximation. After shortly reviewing the pertinent concepts of FRET theory in Sec. II, we discuss in Sec. III how the dipole coupling can be incorporated into the real-time methodology. This leads to a very general scheme for qualitatively checking the validity of the dipole coupling approximation, as demonstrated in Sec. IV. Under certain conditions that are explained in Sec. V one can also determine the coupling matrix element quantitatively. We stress that in all instances we deliberately do not use the Kohn-Sham Slater determinant as an approximation to the true wave function, staying truly on TDDFT grounds.

II. THE DIPOLE COUPLING APPROXIMATION

In the following we briefly review the aspects of Förster theory that are crucial for the further considerations. Starting with Fermi's Golden Rule, the energy transfer rate k^{ET} can be written as [15]

$$k^{\mathrm{ET}} = 2\pi |V|^2 \int_0^\infty d\epsilon \, J(\epsilon), \tag{1}$$

where $J(\epsilon)$ is the spectral overlap between the normalized donor emission and acceptor absorption spectra. Hartree atomic units are used throughout. V is the electronic coupling matrix element

$$V = \langle DA^* | \hat{V}^{\mathrm{C}} | D^* A \rangle, \tag{2}$$

where the Coulomb interaction $\hat{V}^{\mathrm{C}}$ mediates between the initial and final wave functions. Förster theory is based on the assumption that the wave function of the total system can be separated into D and A parts due to negligible electronic coupling between D and A. Initially, the acceptor is in its ground state denoted by $|A\rangle$ and the donor is in an excited

state $|D^*\rangle$. The final wave function corresponds to the inverse situation. Thus, the states in Eq. (2) are written as

$$\begin{aligned}\langle DA^*| &= \frac{1}{\sqrt{2}}(\langle \widetilde{DA^*}| - \langle \widetilde{A^*D}|),\\ |D^*A\rangle &= \frac{1}{\sqrt{2}}(|\widetilde{D^*A}\rangle - |\widetilde{AD^*}\rangle),\end{aligned} \tag{3}$$

where $|\widetilde{DA^*}\rangle$ abbreviates the product state $|D\rangle|A^*\rangle$, respectively. Accordingly, the coupling matrix element splits into the Coulomb contribution (i.e., D and D^* having the same coordinates)

$$V^{\mathrm{C}} = \langle \widetilde{DA^*}|\hat{V}^{\mathrm{C}}|\widetilde{D^*A}\rangle \tag{4}$$

and the so-called exchange contribution

$$V^{x} = \langle \widetilde{A^*D}|\hat{V}^{\mathrm{C}}|\widetilde{D^*A}\rangle \tag{5}$$

(i.e., A^* and D^* having the same coordinates) [14,59,60]. As the overlap between states falls exponentially with increasing R, V^x is neglected in FRET and only the Coulomb term contributes to the Förster rate-of-excitation energy transfer. (The exchange contribution gives the so-called Dexter-type energy transfer [59].)

Under the assumption that the extension of the D and A molecules is small compared to R

$$\frac{|\mathbf{r}^{\mathrm{A}}|}{|\mathbf{R}|} \ll 1 \quad \text{and} \quad \frac{|\mathbf{r}^{\mathrm{D}}|}{|\mathbf{R}|} \ll 1, \tag{6}$$

(see Fig. 1 for the notation), the Coulomb interaction between the electrons of D and A is expanded in a multipole series. Expanding up to powers R^{-3}, the interaction is written as

$$\begin{aligned}&\sum_{j,k} \frac{1}{|\mathbf{R} + (\mathbf{r}_k^{\mathrm{A}} - \mathbf{r}_j^{\mathrm{D}})|}\\ &= \sum_{j,k}\left\{\frac{1}{|\mathbf{R}|} - \frac{(\mathbf{r}_k^{\mathrm{A}} - \mathbf{r}_j^{\mathrm{D}})\mathbf{R}}{|\mathbf{R}|^3} + \frac{3}{2}\frac{\left[(\mathbf{r}_k^{\mathrm{A}} - \mathbf{r}_j^{D})\mathbf{R}\right]^2}{|\mathbf{R}|^5}\right.\\ &\quad \left. - \frac{(\mathbf{r}_k^{\mathrm{A}} - \mathbf{r}_j^{D})^2}{2|\mathbf{R}|^3} + \cdots\right\},\end{aligned} \tag{7}$$

where the k sum runs over all electrons of the acceptor, and the j sum runs over all electrons in the donor. Introducing the orientation factor

$$\kappa^{\mathrm{DA}} = \hat{e}^{\mathrm{D}}\hat{e}^{\mathrm{A}} - 3(\hat{e}^{\mathrm{D}}\mathbf{R})(\hat{e}^{\mathrm{A}}\mathbf{R}), \tag{8}$$

with the vectors $\hat{e}^i = \frac{\mathbf{r}^i}{|\mathbf{r}^i|}$, the transition dipole moments

$$\begin{aligned}\boldsymbol{\mu}^{\mathrm{D}} &= \langle D|\sum_j \mathbf{r}_j^{\mathrm{D}}|D^*\rangle\\ \boldsymbol{\mu}^{\mathrm{A}} &= \langle A|\sum_k \mathbf{r}_k^{\mathrm{A}}|A^*\rangle,\end{aligned} \tag{9}$$

and assuming orthogonality of D and A states, one finds the coupling matrix element of FRET theory

$$V^{\mathrm{FRET}} = \kappa^{\mathrm{DA}}\frac{|\boldsymbol{\mu}^{\mathrm{A}}||\boldsymbol{\mu}^{\mathrm{D}}|}{|\mathbf{R}|^3}. \tag{10}$$

V^{FRET} features the characteristic R^{-3} dependence of Förster theory. Together with Eq. (1) this yields the rate of the Förster-type excitation energy transfer.

III. A DIPOLE COUPLING SCHEME IN THE TDDFT CONTEXT

The previously presented concept relies on using the states $|A\rangle$ and $|D\rangle$. For the typical molecules of interest involving tens to hundreds of electrons, the computational cost of calculating these many-particle states with *ab initio* wave function methods is prohibitive. (TD)DFT allows one to determine the electronic structure of systems of that size, yet again, the many-particle states are not accessible: Even if the ultimate exchange-correlation functional were known, there is no reason to believe that generally the Kohn-Sham Slater determinant will be close to the true correlated wave function. Therefore, a TDDFT scheme that is intended to investigate the dipole coupling approximation that is inherent to Förster theory must be based solely on the variable that is reliable in (TD)DFT, namely the density. One way of how this can be achieved is presented in the following.

The real-time formalism of TDDFT that we want to apply is based on the time-dependent Kohn-Sham (KS) equations [43,45,48,50]

$$i\frac{\partial}{\partial t}\varphi_j(\mathbf{r},t) = h_{\mathrm{KS}}(\mathbf{r},t)\varphi_j(\mathbf{r},t), \tag{11}$$

where h_{KS} is the time-dependent KS Hamiltonian given by

$$h_{\mathrm{KS}}(\mathbf{r},t) = -\frac{\nabla^2}{2} + v_{\mathrm{H}}(\mathbf{r},t) + v_{\mathrm{xc}}(\mathbf{r},t) + v_{\mathrm{ext}}(\mathbf{r},t). \tag{12}$$

The potential $v_{\mathrm{ext}}(\mathbf{r},t)$ represents all external contributions (e.g., nuclei and a laser field). The electron interaction is taken into account via the Hartree potential

$$v_{\mathrm{H}}[n](\mathbf{r},t) = \int \frac{n(\mathbf{r}',t)}{|\mathbf{r}-\mathbf{r}'|}\,d^3r' \tag{13}$$

and the exchange-correlation (xc) potential $v_{\mathrm{xc}}(\mathbf{r},t)$. Whereas $v_{\mathrm{H}}[n](\mathbf{r},t)$ is known explicitly as the functional derivative of the classical Hartree energy

$$E_{\mathrm{H}}[n] = \frac{1}{2}\int \frac{n(\mathbf{r},t)n(\mathbf{r}',t)}{|\mathbf{r}-\mathbf{r}'|}\,d^3r\,d^3r', \tag{14}$$

the xc potential has to be approximated as its exact form is unknown.

The real-time KS equations lend themselves very naturally to a general and straightforward scheme for checking the dipole coupling approximation that is at the heart of FRET: One can explicitly implement the multipole expansion of Förster into the TDDFT equations and compare the orbital propagation with the multipole expansion to another one without (i.e., with the usual full KS Hamiltonian). The details of this strategy are explained in the following.

In accordance with the assumption of an appreciable spatial separation of the D and A systems that is underlying FRET theory, we divide the full density into a D and an A part. For the sake of being as explicit in our notation as possible, we assume in all of the following that the D and A densities

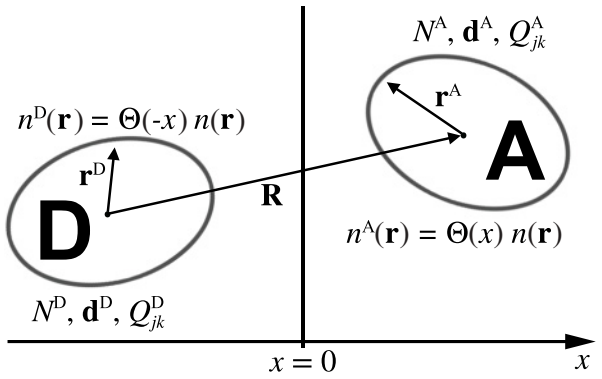

FIG. 1. Donor and acceptor are separated by the distance $R = |\mathbf{R}|$ and can thus be localized in the half-spaces with negative and positive x coordinate, for the sake of an explicit notation. Each system is characterized by its multipole moments N^i, $\mathbf{d}^i$ and Q^i_{jk}, where $i = \{\mathrm{D},\mathrm{A}\}$ labels the system, respectively. Distances with respect to the center of D and A, respectively, are denoted by $\mathbf{r}^\mathrm{D}$ and $\mathbf{r}^\mathrm{A}$.

are localized in the half spaces of negative and positive x coordinates, respectively, as shown in Fig. 1

$$\begin{aligned} n^\mathrm{D}(\mathbf{r}) &= \Theta(-x) n(\mathbf{r}), \\ n^\mathrm{A}(\mathbf{r}) &= \Theta(x) n(\mathbf{r}), \end{aligned} \tag{15}$$

where $\Theta(x)$ is the Heaviside step function.

As reviewed previously, Förster's concept is based on using the exact states for the separate molecules, but only taking the classical (Hartree) interaction between the transition dipoles of D and A into account for the intermolecular coupling. Consequently, a TDDFT analog of Förster's approach should take all electron interaction effects into account [i.e., use v_H and the (unknown) exact v_xc] within each molecule, but use only the Hartree potential for the coupling between D and A, and the latter only to low order in a multipole expansion.

In the following we describe how this expansion can be incorporated into a TDDFT scheme in practice, and we start by noting that there are two possible paths to implement the dipole coupling approximation for the Hartree coupling. The first is to start with the Hartree energy of Eq. (14), perform the multipole expansion, and then take the functional derivative to obtain the potential. The second is to start from the Hartree potential itself and perform the dipole approximation on the level of Eq. (13).

Following the first route, the Hartree energy splits into three components

$$E_\mathrm{H}[n] = E_\mathrm{H}[n^\mathrm{D}] + E_\mathrm{H}[n^\mathrm{A}] + \int \frac{n^\mathrm{A}(\mathbf{r}) n^\mathrm{D}(\mathbf{r}')}{|\mathbf{r}-\mathbf{r}'|}\, d^3r d^3r', \tag{16}$$

where the first two contributions separate in D and A, whereas the third term contains the interaction between the D and A systems. The expansion (7) is used in the third term on the right-hand side (rhs) of Eq. (16) to obtain the Hartree energy E^{dd}_H in the dipole coupling approximation. Calculating the functional derivative of Eq. (16) we use the functional chain rule to take the separation in D and A densities into account

$$v_\mathrm{H}[n](\mathbf{r}) = \sum_{i=\mathrm{D},\mathrm{A}} \int \frac{\delta E^{dd}_\mathrm{H}[n^\mathrm{D},n^\mathrm{A}]}{\delta n^i(\mathbf{r}')} \frac{\delta n^i(\mathbf{r}')}{\delta n(\mathbf{r})}\, d^3r'. \tag{17}$$

Consequently, the potential in the dipole coupling approximation (superscript *dd*) as derived from the energy (thus superscript index E) can be written as

$$\begin{aligned} v^{dd_\mathrm{E}}_\mathrm{H}[n^\mathrm{D},n^\mathrm{A}] = {} & \big(v_\mathrm{H}[n^\mathrm{D}] + v^{dd_\mathrm{E},\mathrm{D}}_\mathrm{H}[n^\mathrm{A}]\big)\Theta(-x) \\ & + \big(v_\mathrm{H}[n^\mathrm{A}] + v^{dd_\mathrm{E},\mathrm{A}}_\mathrm{H}[n^\mathrm{D}]\big)\Theta(x), \end{aligned} \tag{18}$$

where $v_\mathrm{H}[n^{\mathrm{D}(\mathrm{A})}]$ is the Hartree potential of D(A) and $v^{dd_\mathrm{E},\mathrm{D}(\mathrm{A})}_\mathrm{H}[n^{\mathrm{A}(\mathrm{D})}]$ is the potential resulting from the third term of Eq. (16) in the D(A) half-space. With the help of the multipole moments of the D(A) density,

$$\begin{aligned} N^i &= \int n^i(\mathbf{r}^i)\, d^3r^i, \quad \mathbf{d}^i = \int \mathbf{r}^i n^i(\mathbf{r}^i)\, d^3r^i, \\ Q^i_{jk} &= \int n^i(\mathbf{r}^i)\big(3r^i_j r^i_k - {r^i}^2 \delta_{jk}\big)\, d^3r^i, \end{aligned} \tag{19}$$

where $i = \mathrm{D},\mathrm{A}$, the Förster potential that the donor density generates in the half space of A (cf. Fig. 1) is

$$\begin{aligned} v^{dd_\mathrm{E},\mathrm{A}}_\mathrm{H}[n^\mathrm{D}](\mathbf{r}^\mathrm{A}) = {} & \frac{N^\mathrm{D}}{|\mathbf{R}|} - \frac{(N^\mathrm{D}\mathbf{r}^\mathrm{A} - \mathbf{d}^\mathrm{D})\mathbf{R}}{|\mathbf{R}|^3} + \frac{\mathbf{r}^\mathrm{A}\mathbf{d}^\mathrm{D}}{|\mathbf{R}|^3} \\ & + \frac{N^\mathrm{D}}{2} \sum_{j,k=1}^{3} \big(3r^\mathrm{A}_j r^\mathrm{A}_k - {r^\mathrm{A}}^2 \delta_{jk}\big) \frac{R_j R_k}{|\mathbf{R}|^5} \\ & + \sum_{j,k=1}^{3} \frac{Q^\mathrm{D}_{jk} R_j R_k}{2|\mathbf{R}|^5} - \frac{3(\mathbf{R}\mathbf{r}^\mathrm{A})(\mathbf{R}\mathbf{d}^\mathrm{D})}{|\mathbf{R}|^5}. \end{aligned} \tag{20}$$

The corresponding potential $v^{dd_\mathrm{E},\mathrm{D}}_\mathrm{H}[n^\mathrm{A}](\mathbf{r}^\mathrm{D})$ is obtained from Eq. (20) by interchanging the D and A superscripts and replacing $\mathbf{R}$ by $-\mathbf{R}$.

As an alternative to this derivation we can take the second route. To this end we start directly at the level of the potential and write the Hartree potential on the A side as

$$v^\mathrm{A}_\mathrm{H}[n_\mathrm{D},n_\mathrm{A}] = \int \frac{n^\mathrm{A}(\mathbf{r}')}{|\mathbf{r}^\mathrm{A} - \mathbf{r}'|}\, d^3r' + \int \frac{n^\mathrm{D}(\mathbf{r}^\mathrm{D})}{|\mathbf{r}^\mathrm{A} + \mathbf{R} - \mathbf{r}^\mathrm{D}|}\, d^3r^\mathrm{D}. \tag{21}$$

This expression leads to another natural way of translating Förster's Hartree dipole coupling concept into a TDDFT scheme: The contribution from the A density to the Hartree potential in A's own half space is taken into account fully, whereas the contribution from the D density to the Hartree potential in A's half space [the second term on the rhs of Eq. (21)] is expanded in analogy to Eq. (7). The latter leads to the potential

$$v^{dd_v,\mathrm{A}}_\mathrm{H}[n^\mathrm{D}] = \frac{N^\mathrm{D}}{|\mathbf{r}^\mathrm{A} + \mathbf{R}|} + \frac{\mathbf{d}^\mathrm{D}(\mathbf{r}^\mathrm{A} + \mathbf{R})}{|\mathbf{r}^\mathrm{A} + \mathbf{R}|^3} + \sum_{j,k=1}^{3} \frac{Q^\mathrm{D}_{jk} R_j R_k}{2|\mathbf{r}^\mathrm{A} + \mathbf{R}|^5}, \tag{22}$$

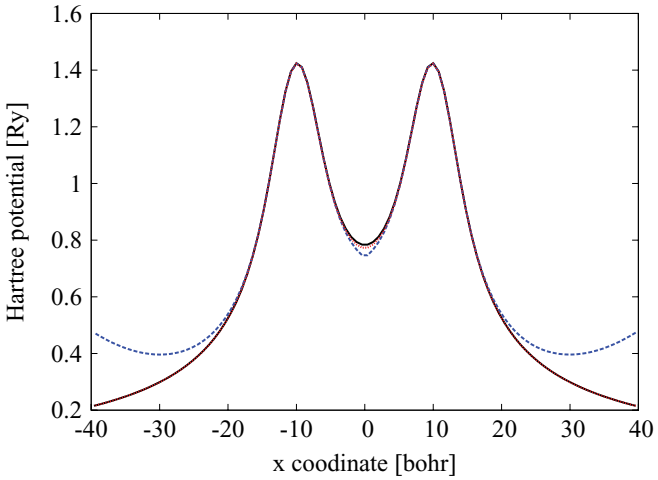

FIG. 2. (Color online) Comparison of the usual Hartree potential $v_{\mathrm{H}}[n]$ (black solid line) with the Hartree potentials $v_{\mathrm{H}}^{dd_v}[n_{\mathrm{D}},n_{\mathrm{A}}]$ (red dotted line) and $v_{\mathrm{H}}^{dd_{\mathrm{E}}}[n_{\mathrm{D}},n_{\mathrm{A}}]$ (blue dashed line). The potentials are plotted along the axis that runs through the centers of the two sodium dimers, while the position of the molecules is -10 and $+10$ bohr.

on the A side (where the superscript index v indicates that we approximated the potential directly, not the energy as in route 1). The corresponding potential on the D side is

$$v_{\mathrm{H}}^{dd_v,\mathrm{D}}[n^{\mathrm{A}}] = \frac{N^{\mathrm{A}}}{|\mathbf{r}^{\mathrm{D}}-\mathbf{R}|} + \frac{\mathbf{d}^{\mathrm{A}}(\mathbf{r}^{\mathrm{D}}-\mathbf{R})}{|\mathbf{r}^{\mathrm{D}}-\mathbf{R}|^3} + \sum_{j,k=1}^{3} \frac{Q_{jk}^{\mathrm{A}} R_j R_k}{2|\mathbf{r}^{\mathrm{D}}-\mathbf{R}|^5}. \tag{23}$$

Using these expressions instead of $v_{\mathrm{H}}^{dd_{\mathrm{E}},\mathrm{A}}$ and $v_{\mathrm{H}}^{dd_{\mathrm{E}},\mathrm{D}}$ in Eq. (18) defines the potential $v_{\mathrm{H}}^{dd_v}$.

Let us pause for a moment to compare the two routes. The first one, starting from the energy, appears more natural if one has in mind Förster's original work, which was based on the energy. However, the second one, directly using the potential, seems to be more natural in the context of KS (TD)DFT in which the potential is readily available. However, both are valid translations of Förster's concept into a real-time TDDFT context, and it is thus not clear *a priori* which one should be preferred. To get a better understanding of the differences between $v_{\mathrm{H}}^{dd_{\mathrm{E}}}$ and $v_{\mathrm{H}}^{dd_v}$ we plot them in Fig. 2 for a transparent example, a system of two sodium dimers [61] aligned in parallel and separated by $R = 20$ a.u..

While $v_{\mathrm{H}}^{dd_v}$ is rather similar to the full Hartree potential, the potential $v_{\mathrm{H}}^{dd_{\mathrm{E}}}$ is considerably too low in the central region between the dimers and rises unphysically far away from the dimers. This behavior can be traced back to the fact that, in calculating $v_{\mathrm{H}}^{dd_{\mathrm{E}}}$, we always divide by powers of the fixed R [see denominators of Eq. (20)] while the numerators rise with growing distance r to the corresponding molecule. In contrast, in potential $v_{\mathrm{H}}^{dd_v}$ the distance r enters in the denominator. Therefore, $v_{\mathrm{H}}^{dd_v}$ decays with the growing distance to the corresponding dimer. As this is the behavior one naturally expects from a potential, we used $v_{\mathrm{H}}^{dd_v}$ in our calculations [62].

IV. REAL-TIME INVESTIGATION OF THE DIPOLE COUPLING APPROXIMATION

Our focus so far was on the conceptual work of translating Förster's dipole coupling idea into the (TD)DFT context. For using the scheme in practical calculations, we have to address the question of which influences the approximation that is used for the description of the xc effects will have.

The excitation spectrum of two identical molecules at a separation large enough for the individual molecular densities to not overlap can qualitatively be described as being similar to the spectrum of a single molecule, but with possibly an energetic splitting of the monomer excitations (Davydov splitting, see Sec. V), and with additional charge-transfer excitations from one monomer to the other that carry practically zero oscillator strength.

It is a well known problem of many commonly used density functionals, in particular (semi)local ones, that they seriously underestimate the energy of charge-transfer excitations. In the KS framework, this failure is closely related to the absence of step-like structures in the xc potential that result from discontinuities [63] in TDDFT, see Ref. [64] for a detailed discussion. It has been shown that xc approximations using a large fraction of exact exchange [39], or range-separated hybrid functionals [65], or self-interaction corrections [66] can describe charge transfer well. Using a functional that accurately describes charge transfer is mandatory for an accurate description of two monomers at close distance [67].

In the propagation setup the movement of charge is recorded in real-time and this can be used to directly monitor for charge transfer from one molecule to the other. This built-in warning allows one to check against leaving the "large separation" situation which was described in Sec. II and which is the focus of interest here [68]. At large separation, the energy transfer is completely dominated by the Hartree coupling. It remains mandatory in any case that the xc functional approximation one uses describes the excitation spectrum of the single molecules with reasonable accuracy, as otherwise the time-dependent density and transition dipoles will be incorrect.

Starting from two molecules at a large separation R and decreasing the distance, our aim is to check when the dipole coupling approximation breaks down. Our calculations are performed with our real-time TDDFT extension [51,52] of the real-space code PARSEC [69]. The two molecules are placed in two different half-spaces of the real-space grid. All investigations are performed in the so-called supermolecular approach [70], where we consider D and A as a combined system. To distinguish between a coupling of excited states that fulfills the assumptions leading to expansion (7) and a coupling that does not, we compare the time-dependent dipole moments of D and A obtained by a DFT plus TDDFT run with the full Hartree potential, to the ones obtained in a second run using the potential $v_{\mathrm{H}}^{dd_v}$. The dipole moments are calculated using the D and A centers of density in the DFT ground state as reference points.

Our proceeding is as follows: (1) determine the spectrum of one single molecule, (2) choose the excitation of interest, (3) perform a real-time TDDFT calculation using the full Hartree potential with a short laser pulse as the initial excitation, (4) repeat step (3) with $v_{\mathrm{H}}^{dd_v}$, (5) compare the

time-dependent dipole moments obtained in steps (3) and (4). The laser pulse is added as an external potential during the first steps of the real-time propagation only within the half-space of D. The frequency, length, and shape of the pulse are tuned to excite the system only in a narrow frequency band around the excitation chosen in step (2). (See Appendix A for details.)

In the following we demonstrate the use of this approach in calculations for dimers of Na_2 and C_7H_6O, respectively. These systems are transparent enough to allow for a clear explanation and demonstration of our concept and they are established reference systems [36,71]. We employ the time-dependent local density approximation (TDLDA) as it well describes the excitations of Na_2 and C_7H_6O [72,73] that are of interest in our study. The possible underestimation of charge-transfer excitations that was discussed at the beginning of this section is not of concern here as we are specifically interested in the major excitations carrying dipole oscillator strength. These are described well by TDLDA for the systems that we study.

We first investigate the coupling between two sodium dimers with parallel alignment of the two Na_2 axes as a function of the distance R between the two Na_2 molecules. As the excitation of interest we choose the one that is at 2.1 eV in the Na_2 spectrum [71,72]. A typical time evolution of the acceptor dipole moment is shown in Fig. 3. At the chosen distance, $R = 15$ bohr, there are obvious deviations between the time-dependent dipole moment that is obtained using the full Hartree potential and the one that is obtained using $v_{\mathrm{H}}^{dd_v}$.

The deviations are a manifestation of the breakdown of the dipole coupling approximation at 15 bohr. A systematic analysis of the deviations in the dipole moment at a range of distances from 45 to 15 bohr is depicted in Fig. 4. Qualitatively, we see in Fig. 4 three regimes: For very large distances (45 and 35 bohr) the differences vanish and one is clearly in the dipole regime. At smaller distances (around 25 bohr in the present example) one starts to observe deviations, and for yet smaller distances (15 bohr) the dipole moments differ very significantly during their time evolution—although the density overlap is still small. Here the dipole approximation clearly fails and higher multipoles are relevant.

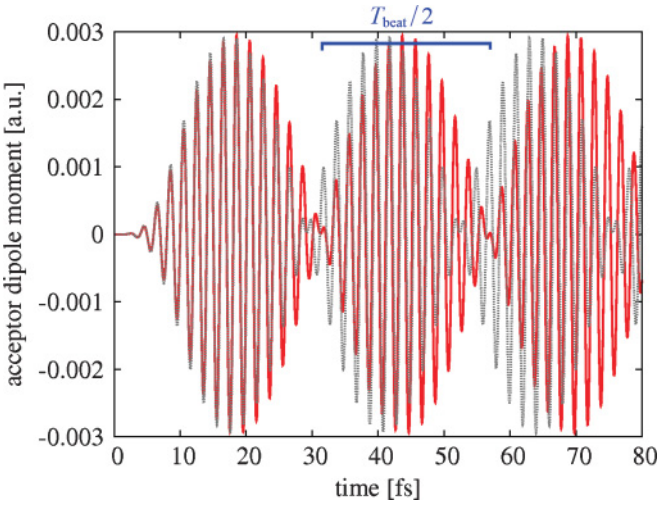

FIG. 3. (Color online) Acceptor dipole moment along the Na_2 molecular axis, recorded as a function of time, for a system of two Na_2 with a separation of $R = 15$ bohr. The time evolution was calculated using the full Hartree potential (solid, red) and the potential $v_{\mathrm{H}}^{dd_v}$ (dotted, black). The coupling between D and A manifests itself in the beat frequency ω_{beat} of an oscillation between D and A (cf. Sec. V). This beat frequency can be extracted from the A dipole moment via $\omega_{\mathrm{beat}} = 2\pi/T_{\mathrm{beat}}$.

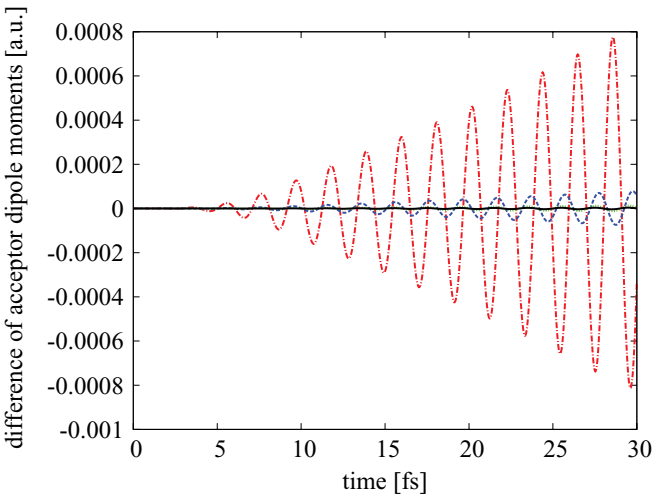

FIG. 4. (Color online) Difference between the acceptor dipole moments obtained in a calculation using the full Hartree potential and another one using $v_{\mathrm{H}}^{dd_v}$ for an Na_2 dimer, for different values of R: 15 bohr (dot dashed, red), 25 bohr (dashed, blue), 35 bohr (dotted, green) and 45 bohr (solid, black).

The same effects are seen in the second example in which we examine the coupling between two C_7H_6O molecules that are aligned in parallel as depicted in Fig. 5. We again focus on the lowest excitation with appreciable oscillator strength. The dipole moment time evolution was calculated for a range of distances from $R = 40$ bohr to $R = 12$ bohr, again using the two different potentials as discussed previously. Characteristic results (distances of 24 to 12 bohr) are shown in Fig. 6. The differences at $R = 12$ bohr and $R = 16$ bohr significantly exceed the differences at the larger separations. Therefore, one can argue qualitatively that up to 16 bohr separation one cannot speak of a Förster-type coupling. From 20 bohr on, the differences in the dipole moment time evolution are notably smaller and the Förster-type dipole approximation can be considered valid [74].

As our analysis has so far focused on the total dipole moments, it is rather general and the concept can

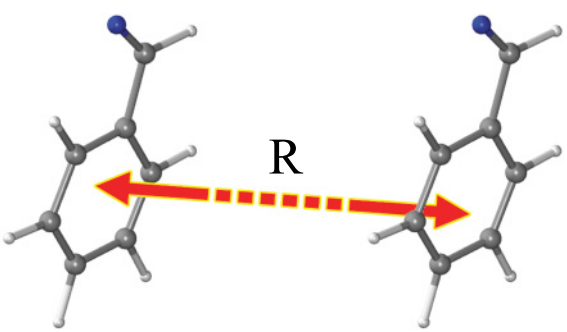

FIG. 5. (Color online) System of two C_7H_6O molecules, where the distance R is varied from 40 to 12 bohr.

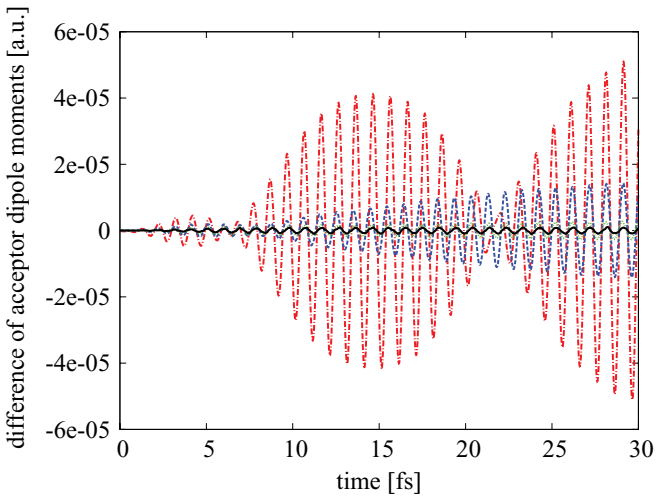

FIG. 6. (Color online) Difference of acceptor dipole moment in a system of two C_7H_6O between a calculation using the full Hartree potential and another one with the potential $v_H^{dd_v}$. The molecules are separated by 12 bohr (dot dashed, red), 16 bohr (dashed, blue), 20 bohr (dotted, green), and 24 bohr (solid, black).

straightforwardly be extended, e.g. to unequal dimers. Comparing characteristic features of the dipole moment evolution obtained with full coupling and with dipole coupling, one can assess the trust range of the dipole approximation.

If the excitations of interest have the special feature of being rather well separated from all other excitations so that one can think about the coupling as a coupling in a two-level system, then one can also determine the coupling matrix element quantitatively from the TDDFT calculation—despite the fact that one does not explicitly know the states in TDDFT. This is the topic of the next section.

V. EXTRACTING THE COUPLING MATRIX ELEMENT FROM A REAL-TIME PROPAGATION

A coupling matrix element of type (2) enters the energy transfer rate (1), and it is a close-lying question whether and how it can be evaluated. In principle, one could calculate the initial and final states and evaluate Eq. (2) directly. However, as discussed previously, the states are hard to compute from first principles and there is no rigorous reason to identify the KS Slater determinant with the true wave function. Therefore, if one wants to stay on the safe formal grounds of (TD)DFT by not using the KS Slater determinant as an approximation to the true wave function, one has to think about alternative ways to determine the coupling matrix element.

The Davydov splitting [75–77] is such an alternative [34–39,41]. In the case of two equal molecules, the Davydov splitting $\Delta\Omega$ equals the energy splitting ΔE of the (nearly) degenerate excitation energies of the monomers in the supermolecule [34,36,37,39]. In the discussed situation $\Delta\Omega$ is proportional to the coupling matrix element (2)

$$V = \frac{\Delta\Omega}{2}. \tag{24}$$

This observation can be exploited in TDDFT by calculating the spectrum [50,78–80] and deducing the coupling matrix element from the energy splitting. In the real-time approach to TDDFT spectra are usually determined by initially exciting the system with a momentum boost [45,81], propagating the time-dependent KS equations [82] using the dipole moment as observable, and calculating the dipole spectrum via a Fourier transformation [81]. As the energy splitting is typically much smaller than the excitation energies themselves, high resolution and thus comparably long propagation times are needed to resolve the splitting.

Therefore, we consider an alternative way of extracting the relevant information by observing the D and A dipole moments separately. It considerably reduces the computational load. We note that the Davydov splitting $\Delta\Omega$ and consequently also the coupling matrix element V manifests itself as a frequency ω_{beat} in the time-dependent D (and A) dipole moment. This frequency can be extracted as a beat frequency ω_{beat} of an oscillation between D and A. (See Appendix B for details.) From it one obtains

$$V = \omega_{\text{beat}}. \tag{25}$$

Apart from the beat the dipole moment of the system oscillates only at frequencies close to the laser frequency that was used for the excitation. Hence the beat frequency can be determined easily from the D and A dipole moments (see Fig. 3). The essential observation now is that for doing so, the dipole moment time evolution only has to be recorded long enough to capture one half cycle of the beat. This is a much shorter time than the time needed to obtain an accurate spectrum from the Fourier transformation. Thus, the coupling strength can be determined with moderate simulation times.

We used this approach to determine the coupling of the lowest excitation of the two sodium dimers. Figure 7 shows the thus obtained distance dependence of the coupling matrix element. One observes significant differences from the dipole

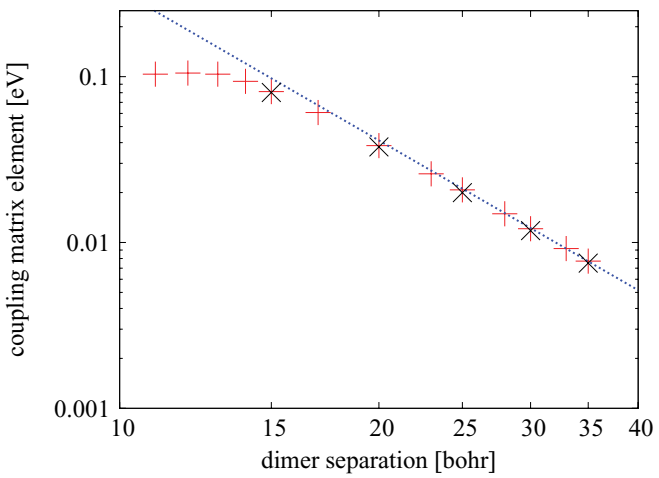

FIG. 7. (Color online) Coupling matrix element between the excited states at 2.1 eV of two Na_2 versus the dimer separation. Red crosses show the results from our real-time and real-space implementation. As a guide to the eye we plotted a dotted line with slope -3 which corresponds to a Förster-type coupling. As a confirmation of our implementation we also report results that we obtained using linear response TDDFT from a commercial program package [83–85] (black crosses).

coupling behavior for distances below 20 bohr. Above 25 bohr the coupling falls with the expected $1/R^{-3}$ dependence.

As a test of our real-time and real-space implementation we followed Ref. [39] and computed linear response TDDFT spectra for a couple of dimer distances with the TURBOMOLE package [83–85] using the local density approximation and Fully Optimized Contracted Gaussian Basis Sets of Triple Zeta Valence Quality (def2-TZVP) [86]. The coupling matrix elements (see Fig. 7) are calculated according to Eq. (24) exploiting the Davydov splitting. The agreement between the two methods is very good and the observed small differences can be attributed to technical differences such as the use of pseudopotentials and basis sets versus real space.

For putting our findings into perspective one should compare the distance of 25 bohr to the bond length of the sodium dimer, which is 5.78 bohr. The ratio of the extension of the molecular systems to their separation indicates that one has to be careful in relying on the dipole coupling approximation for extended systems that are not very far apart.

VI. CONCLUSION

We have presented a qualitative and a quantitative scheme for investigating the coupling behavior of two molecules within the real-time approach to TDDFT. The approach allows one to distinguish between a Förster-type dipole coupling and a non-dipole coupling on very general grounds. If the coupled excitations that are of interest can be considered as a two-level system (i.e., large energetic separation from other excitations), then the coupling matrix element can be determined efficiently in the real-time scheme by evaluating the Davydov splitting from a beat frequency.

Already the small molecules investigated in this manuscript show notable deviations from the Förster-type dipole coupling at moderate distances. For larger molecules such as typically used for spectroscopic labeling or in molecular electronics, the question at which distances FRET can be relied on is thus of great significance. Theoretical tools such as the one discussed here can play an important role, as they enable us to check whether the FRET dipole coupling approximation can be applied or not.

ACKNOWLEDGMENTS

Financial support by the DFG and the Elitestudienprogramm "Macromolecular Science" is gratefully acknowledged.

APPENDIX A: EXCITATION WITH A LASER PULSE

Here we briefly explain how we excite the system by a laser pulse in the real-time investigation of the dipole coupling approximation in Sec. IV. The laser acts as a time-dependent external potential in dipole approximation

$$E_L(t) = E_{\mathrm{env}}(t)\sin(\omega_L t), \tag{A1}$$

where $E_{\mathrm{env}}(t)$ is the pulse envelope. The frequency ω_L of the pulse was chosen to equal the excitation energy we were interested in. We used the envelope $E_{\mathrm{env}}(t) = E_{\max}\sin^2(\frac{\pi t}{T_L})$ as this form leads to a Fourier spectrum in which the side maxima are much lower than the main peak (typically the height of the first side maximum is less than 3% of the height of the main peak). The length T_L of the pulse is tuned by comparing the Fourier spectrum of the pulse with the excitation spectrum of the molecule: T_L was chosen such that the first side maximum of the pulse's spectrum lay closer to the pulse's main frequency than the neighboring peak in the molecule's excitation spectrum. In all cases we investigated, the excitations of the single molecules were sufficiently separated from each other to dominantly excite just one excited state of the system. This could be verified from the time-dependent dipole signal.

APPENDIX B: BEAT OSCILLATION IN THE TIME-DEPENDENT ACCEPTOR DIPOLE MOMENT

In this Appendix we briefly explain why ω_{beat} can be extracted from the dipole moment. We start by noting that Eq. (24) is derived in a two-state model [35,36], where $|\widetilde{D^*A}\rangle$ and $|\widetilde{DA^*}\rangle$ are a pair of resonant states. The time evolution

$$|\Psi(t)\rangle = a_1(t)|\widetilde{D^*A}\rangle + a_2(t)|\widetilde{DA^*}\rangle, \tag{B1}$$

of the two-state system with initial state $|\Psi(0)\rangle = |\widetilde{D^*A}\rangle$ is given by the coefficients $a_1(t)$ and $a_2(t)$ [87]

$$\begin{aligned} |a_1(t)|^2 &= \cos^2(Vt), \\ |a_2(t)|^2 &= \sin^2(Vt). \end{aligned} \tag{B2}$$

The coefficients oscillate with the beat frequency ω_{beat}, see Eq. (25). The corresponding time-dependent dipole moment $\mathbf{d}^{\mathrm{A}}(t) = \langle\Psi(t)|\mathbf{r}^{\mathrm{A}}|\Psi(t)\rangle$ on the A side can be calculated as

$$\mathbf{d}^{\mathrm{A}}(t) = |a_1(t)|^2\langle A|\mathbf{r}^{\mathrm{A}}|A\rangle + |a_2(t)|^2\langle A^*|\mathbf{r}^{\mathrm{A}}|A^*\rangle, \tag{B3}$$

where we exploited the orthogonality of $|D\rangle$ and $|D^*\rangle$. If the static dipole moment $\langle A|\mathbf{r}^{\mathrm{A}}|A\rangle$ of A vanishes, (B3) simplifies to

$$\mathbf{d}^{\mathrm{A}}(t) = |a_2(t)|^2\langle A^*|\mathbf{r}^{\mathrm{A}}|A^*\rangle. \tag{B4}$$

Therefore, the resonance oscillation of the coefficients can be observed in the time evolution of the dipole moment $\mathbf{d}^{\mathrm{A}}(t)$. Both Eqs. (B3) and (B4) can be used to determine the coupling matrix element V via the beat frequency (25).

[1] Y.-C. Cheng and G. R. Fleming, Annu. Rev. Phys. Chem. **60**, 241 (2009).
[2] S. Tretiak and S. Mukamel, Chem. Rev. **102**, 3171 (2002).
[3] B. Kippelen and J.-L. Brédas, Energy Environ. Sci. **2**, 251 (2009).
[4] C. W. Tang, Appl. Phys. Lett. **48**, 183 (1986).
[5] J. I. Basham, G. K. Mor, and C. A. Grimes, ACS Nano **4**, 1253 (2010).
[6] R. H. Friend *et al.*, Nature (London) **397**, 121 (1999).
[7] G. D. Scholes, Chem. Phys. **275**, 373 (2002).

[8] G. D. Scholes and G. R. Fleming, J. Phys. Chem. B **104**, 1854 (2000).
[9] X. Hu, A. Damjanović, T. Ritz, and K. Schulten, Proc. Natl. Acad. Sci. USA. **95**, 5935 (1998).
[10] M. D. Newton, Chem. Rev. **91**, 767 (1991).
[11] S. Speiser, Chem. Rev. **96**, 1953 (1996).
[12] Th. Förster, Naturwiss. **33**, 166 (1946).
[13] Th. Förster, Ann. Phys. (NY) **437**, 55 (1948).
[14] Th. Förster, in *Modern Quantum Chemistry*, edited by O. Sinnanoglu (Academic Press, New York, 1965), Vol. 3, pp. 93–137.
[15] G. D. Scholes, Annu. Rev. Phys. Chem. **54**, 57 (2003).
[16] R. Métivier, F. Nolde, K. Müllen, and T. Basché, Phys. Rev. Lett. **98**, 047802 (2007).
[17] Ch. Scharf *et al.*, Chem. Phys. **328**, 403 (2006).
[18] P. Bauer, H. Wietasch, S. M. Lindner, and M. Thelakkat, Chem. Mater. **19**, 88 (2007).
[19] T. Körzdörfer, S. Tretiak, and S. Kümmel, J. Chem. Phys. **131**, 034310 (2009).
[20] F. Laquai, Y.-S. Park, J.-J. Kim, and T. Basché, Macromol. Rapid Commun. **30**, 1203 (2009).
[21] D. Beljonne, C. Curutchet, G. D. Scholes, and R. J. Silbey, J. Phys. Chem. B **113**, 6583 (2009).
[22] L. Stryer and R. P. Haugland, Proc. Natl. Acad. Sci. USA **58**, 719 (1967).
[23] L. Stryer, Annu. Rev. Biochem. **47**, 819 (1978).
[24] R. Ziessel, M. A. H. Alamiry, K. J. Elliott, and A. Harriman, Angew. Chem. Int. Ed. **48**, 2772 (2009).
[25] S. E. Braslavsky *et al.*, Photochem. Photobiol. Sci. **7**, 1444 (2009).
[26] K. F. Wong, B. Bagchi, and P. J. Rossky, J. Phys. Chem. A **108**, 5752 (2004).
[27] H. Singh and B. Bagchi, Curr. Sci. **89**, 1710 (2005).
[28] Y. R. Khan, T. E. Dykstra, and G. D. Scholes, Chem. Phys. Lett. **461**, 305 (2008).
[29] E. Dolghih *et al.*, J. Phys. Chem. A **113**, 4639 (2009).
[30] S. Saini, H. Singh, and B. Bagchi, J. Chem. Sci. **118**, 23 (2006).
[31] S. Saini, S. Bhowmick, V. B. Shenoy, and B. Bagchi, J. Photochem. Photobiol. A: Chem. **190**, 335 (2007).
[32] R. Baer and E. Rabani, J. Chem. Phys. **128**, 184710 (2008).
[33] H. Tamura, J.-M. Mallet, M. Oheim, and I. Burghardt, J. Phys. Chem. C **113**, 7548 (2009).
[34] C.-P. Hsu, G. R. Fleming, M. Head-Gordon, and T. Head-Gordon, J. Chem. Phys. **114**, 3065 (2000).
[35] C.-P. Hsu, J. Chin. Chem. Soc. **50**, 745 (2003).
[36] J. Neugebauer, J. Chem. Phys. **126**, 134116 (2007).
[37] J. Neugebauer, J. Phys. Chem. B **112**, 2207 (2008).
[38] B. Fückel *et al.*, J. Chem. Phys. **128**, 074505 (2008).
[39] E. Sagvolden, F. Furche, and A. Köhn, J. Chem. Theory Comput. **5**, 873 (2009).
[40] A. Muñoz-Losa, C. Curutchet, I. F. Galván, and B. Mennucci, J. Chem. Phys. **129**, 034104 (2008).
[41] C. Curutchet *et al.*, J. Chem. Theory Comput. **5**, 1838 (2009).
[42] M. E. Casida, in *Recent Advances in Density Functional Methods, Part I*, edited by D. P. Chong (World Scientific, Singapore, 1995), Vol. 1, Chap. 5, pp. 155–192.
[43] E. K. U. Gross, J. F. Dobson, and M. Petersilka, in *Density Functional Theory*, edited by R. F. Nalewajski, Top. Curr. Chem. (Springer, Berlin, 1996), Vol. 181, p. 81.
[44] C. A. Ullrich, S. Erhard, and E. K. U. Gross, in *Super Intense Laser Atom Physics IV*, Nato ASI series 3/13, edited by H. G. Muller and M. V. Fedorov (Kluwer, Dordrecht, 1996), p. 267.
[45] K. Yabana and G. F. Bertsch, Phys. Rev. B **54**, 4484 (1996).
[46] U. Saalmann and R. Schmidt, Z. Phys. D: At. Mol. Clusters **38**, 153 (1996).
[47] X.-M. Tong and S.-I. Chu, Phys. Rev. A **55**, 3406 (1997).
[48] K. Yabana and G. F. Bertsch, Int. J. Quantum Chem. **75**, 55 (1999).
[49] F. Calvayrac, P.-G. Reinhard, E. Suraud, and C. A. Ullrich, Phys. Rep. **337**, 493 (2000).
[50] M. A. L. Marques and E. K. U. Gross, Annu. Rev. Phys. Chem. **55**, 427 (2004).
[51] M. Mundt and S. Kümmel, Phys. Rev. B **76**, 035413 (2007).
[52] M. Mundt, J. Theor. Comput. Chem. **8**, 561 (2009).
[53] J. R. Chelikowsky, L. Kronik, and I. Vasiliev, J. Phys. Condens. Matter **15**, R1517 (2003).
[54] M. A. L. Marques, X. Lopez, D. Varsano, A. Castro, and A. Rubio, Phys. Rev. Lett. **90**, 258101 (2003).
[55] M. A. L. Marques, A. Castro, G. F. Bertsch, and A. Rubio, Comput. Phys. Commun. **151**, 60 (2003).
[56] M. A. L. Marques, A. Castro, and A. Rubio, J. Chem. Phys. **115**, 3006 (2001).
[57] M. Mundt and S. Kümmel, Phys. Rev. A **74**, 022511 (2006).
[58] H. O. Wijewardane and C. A. Ullrich, Phys. Rev. Lett. **100**, 056404 (2008).
[59] D. L. Dexter, J. Chem. Phys. **21**, 836 (1953).
[60] C.-P. Hsu, Acc. Chem. Res. **42**, 509 (2009).
[61] Norm conserving pseudopotentials of Troullier-Martins [N. Troullier and J. L. Martins, Phys. Rev. B **43**, 1993 (1991)] type were used.
[62] In test calculations the actual differences that we observed in the dynamics when using either $v_{\mathrm{H}}^{dd_v}$ or $v_{\mathrm{H}}^{dd_E}$ were rather small. This was a consequence of low density in the regions of space where the two approximations differ.
[63] M. Mundt and S. Kümmel, Phys. Rev. Lett. **95**, 203004 (2005).
[64] S. Kümmel and L. Kronik, Rev. Mod. Phys. **80**, 3 (2008).
[65] T. Stein, L. Kronik, and R. Baer, J. Am. Chem. Soc. **131**, 2818 (2009).
[66] T. Körzdörfer, M. Mundt, and S. Kümmel, Phys. Rev. Lett. **100**, 133004 (2008).
[67] Charge-transfer states may also play a role at large separation if they enter, e.g., as pathways that are not optically excited. In our study here we focus on optical excitation.
[68] As local approximations always underestimate the charge-transfer excitation energy, one will see the charge transfer earlier when using local functionals than it occurs in nature (i.e., one will be warned when monitoring the charge in the real-time approach).
[69] L. Kronik *et al.*, Phys. Status Solidi B **243**, 1063 (2006).
[70] D. Beljonne *et al.*, J. Chem. Phys. **112**, 4749 (2000).
[71] I. Vasiliev, S. Öğüt, and J. R. Chelikowsky, Phys. Rev. Lett. **82**, 1919 (1999).
[72] S. Kümmel, K. Andrae, and P.-G. Reinhard, Appl. Phys. B **73**, 293 (2001).
[73] The change in the excitation energies when going from TDLDA to a functional including a percentage of exact exchange [time-dependent Becke three-parameter Lee-Yang-Parr hybrid

functional (TDB3LYP)] are of the order of 0.2 eV for the excitations of C_7H_6O that carry appreciable oscillator strength. As charge-transfer excitations would be more sensitive to the fraction of the Fock exchange this is another confirmation for the fact that we are not looking at charge-transfer excitations.

[74] We checked up to a separation of 40 bohr that the differences in the dipole moment decrease continuously.

[75] A. S. Davydov, *Quantenmechanik* (Dt. Verl. der Wiss., Berlin, 1967), p. 519.

[76] A. S. Davydov, Phys. Status Solidi **30**, 357 (1968).

[77] M. Kasha, H. R. Rawls, and M. Ashraf El-Bayoumi, Pure Appl. Chem. **11**, 371 (1965).

[78] M. Petersilka, U. J. Gossmann, and E. K. U. Gross, Phys. Rev. Lett. **76**, 1212 (1996).

[79] H. Appel, E. K. U. Gross, and K. Burke, Phys. Rev. Lett. **90**, 043005 (2003).

[80] P. Elliott, K. Burke, and F. Furche, arXiv:cond-mat/0703590.

[81] F. Calvayrac, P. G. Reinhard, and E. Suraud, Ann. Phys. **255**, 125 (1997).

[82] A. Castro, M. A. L. Marques, and A. Rubio, J. Chem. Phys. **121**, 3425 (2004).

[83] TURBOMOLE V6.0 2009, a development of the University of Karlsruhe and Forschungszentrum Karlsruhe GmbH, 1989–2007, TURBOMOLE GmbH, since 2007; available from [http://www.turbomole.com].

[84] R. Ahlrichs, M. Baer, M. Haeser, H. Horn, and C. Koelmel, Chem. Phys. Lett. **162**, 165 (1989).

[85] F. Furche and D. Rappoport, in *Computational Photochemistry*, Theoretical and Computational Chemistry, edited by M. Olivucci (Elsevier, Amsterdam, 2005), Vol. 16, Chap. III.

[86] A. Schäfer, C. Huber, and R. Ahlrichs, J. Chem. Phys. **100**, 5829 (1994).

[87] C. Cohen-Tannoudji, B. Diu, and F. Laloë, *Quantenmechanik Band 1* (Walter de Gruyter, Berlin, 2009) p. 374.